Temporal and Spatio-temporal domains for Neuromorphic Tactile Texture Classification

George Brayshaw
Bristol Robotics Laboratory
University of Bristol
Bristol, United Kingdom
george.brayshaw@brl.ac.uk

Benjamin Ward-Cherrier
Department of Engineering Mathematics
University of Bristol
Bristol, United Kingdom
b.ward-cherrier@bristol.ac.uk

Martin J. Pearson
Bristol Robotics Laboratory
University of the West of England
Bristol, United Kingdom
martin.pearson@brl.ac.uk

***Abstract*—The development of upper limb prosthesis that are able to relay information on their status back to the user is an important step towards making this assistive technology more intuitive. Applied within this context, neuromorphic hardware has the potential to reduce processing time while simultaneously reducing power requirements. Towards this, we have begun a systematic evaluation of algorithms that best leverage rich neuromorphic data, and how such algorithms may be implemented. In this paper, we apply conventional machine learning techniques to temporal domain representations of textures derived from a neuromorphic tactile sensor. We then contrast these results with those from a novel spatio-temporal domain classification approach, the Hierarchy of Event-Based Time-Surfaces (HOTS). We achieved higher accuracies when classifying temporal data with our supervised learning methods (91% with a KNN) than when classifying with HOTS (76% with a single layer), indicating that simple temporal encoding is sufficient for the classification of texture.**

I. Introduction

The human sense of touch is paramount to the way in which we interact with the world around us. The identification of textures is an important aspect of our active sensing and approach to manipulation tasks [1]. Heterogeneous populations of subcutaneous mechanoreceptors work in tandem to generate this important tactile information. There is a high density of these mechanoreceptors within the skin of the hand, particularly at the finger tip, providing the tactile feedback we use to interact with and manipulate objects [2]. The sensation of texture is encoded in the spiking pattern of mechanoreceptors and thus, decoding these patterns is how we infer details from our surroundings. Furthermore, identifying potentially noxious surfaces quickly, as humans do, would help autonomous robotic manipulators, including active prosthesis, to avoid damage.

Neuromorphic systems seek to emulate the spiking behaviour of biological neurons and introduce potential improvements in computing speed and power efficiency when processing data [3]. For these reasons, the use of neuromorphic technology has been promoted by Tavanaei et al. as an energy efficient alternative to widely used convolutional neural networks (CNNs) [4]. Taking a neuromorphic approach to texture detection specifically, allows us to create systems capable of human-level performance on texture identification tasks, as well as exploring neuroscientific theories in order to learn more about how these processes may occur within the human brain.

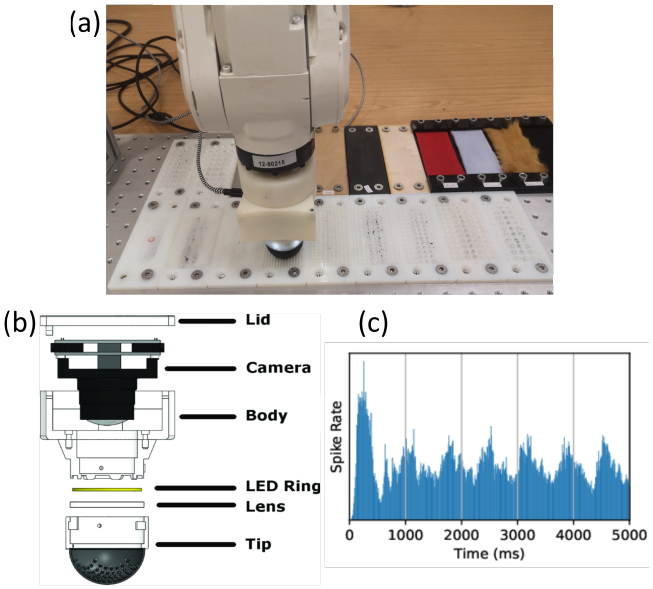

Fig. 1: Experimental setup: (a) the ABB (IRB 120) industrial robotic arm sliding the neuroTac sensor (49 taxels with 2.5mm spacing) across the surface of each artificial texture (shown in white) with uniform pressure. (b) an exploded view of the neuroTac optical sensor [5]. (c) peristimulus time histogram (PTSH) showing the cumulative spike rate of the neuroTac in response to repeated presentations of a typical artificial texture.

Texture sensing and processing has myriad applications throughout the field of robotics, namely complex manipulation tasks and prosthetics. A forecast increase in upper limb loss by 2050 [6] creates a more urgent need for advanced tactile prostheses that are able to relay sensory information to the user. Active prostheses stand to gain from the previously mentioned benefits of neuromorphic design in a number of ways. Current generation active prosthesis are often heavier than the biological arm of the intended user [7]. The introduction of neuromorphic hardware reduces power requirements [8] and therefore battery size, leading to lighter, more intuitive prosthesis. The need for users to be able to react quickly to noxious

touch sensations further supports the use of neuromorphic algorithms, due to their potential for faster processing [9].

While the use of neuromorphic texture classification has been explored previously [5], [10], [11], a direct comparison of different classification methods for neuromorphic data, using the same tactile sensor for each, is yet to be presented. Within this paper we present the results from the following:

1) The application of supervised machine learning methods for classification of two neuromorphic datasets, using time-dependent firing rates.
2) The application of a state of the art spatio-temporal classification algorithm (HOTS) to two neuromorphic datasets.
3) A comparison of these algorithms for the classification of tactile texture data.

II. Related Works

A. Texture Classification

Research is ongoing into tactile sensors with varying levels of complexity and methods of detection [12]–[15]. Many tactile sensors look to mimic the role of the mechanoreceptors within human skin, making them ideal for the collection of texture data. Non-spiking tactile sensors often require the further extraction of features from their output in order to format data for supervised learning. Although these sensors often report high performance when using supervised machine learning techniques [16], [17], the additional computational overheads detract from their utility for real-time classification.

Unsupervised learning methods have also been applied to texture classification tasks [10]. This work achieved a high accuracy of $mean = 86.46$, albeit on a small number of textures ($n = 3$). The conversion of sensor output data to neuromorphic data, however, increases computational overheads and processing time.

Rongala et al. [18] have previously shown that neuromorphic encoding methods can be robust by maintaining high accuracies (97) in a variety of sensing conditions. They did so by using neuromorphic encoding combined with delays in spiking neural networks. We opted to explore the performance of HOTS on texture classification to distinguish the temporal and spatial aspects of the spikes produced.

Our research uses the neuroTac [5], a neuromorphic version of the TacTip tactile sensor [14]. This optical sensor utilises an array of markers (taxels) on the inside of a compliant tip. The deformation of these taxels is monitored by an event-based camera (Davis240, iniVation) which produces a spiking output for each individual pixel, in a process akin to that of natural mechanoreceptors. The spiking events produced by the neuroTac are in the Address Event Representation (AER) data format, and include both a spatial (pixel location) and temporal (event time in microseconds) component [19].

The use of this sensor and the application of the HOTS classification architecture differentiates our research from previous studies into neuromorphic texture classification. While [5] was conducted as an initial investigation into data analysis with the neuroTac, our work looks to utilise its data with different methods of classification. This includes using a spiking neural network (SNN) (HOTS). We validate our approach on both artificial and natural textures and investigate the spatio-temporal characteristics of neuromorphic tactile data produced by the neuroTac.

B. Psychophysical Baseline

A psychophysical baseline against which to compare the performance of our trialled classification methods was selected based on research into similar texture classification experiments with human participants [20]–[22]. An accuracy of $83\% \pm 3\%$ mean standard deviation, was recorded by Delhaye et al. for human participants ($n = 5$) asked to classify 9 textures moving against their skin at a constant speed. Lower performances were found by Chun et al, with a mean accuracy of 57.8% presented ($n = 50$), albeit when participants were asked to classify 12 natural textures. A study by Amini, Lipton and Rus had participants ($n = 10$) classifying 3 different textures, both absolutely and relatively to a prior texture. Using their average results for absolute classification we find their subjects gave an accuracy of $\approx 72\%$. Based on these studies we have concluded on a baseline of 65% to be an appropriate baseline against which to appraise our investigated classifiers. This decision was made to align more with the Chun et al study due to its higher number of participants and similar number of trialled textures. Although we increased the performance of our baseline slightly to account for the reduction in number of textures and the artificial nature of our textures.

Despite the sources cited above, there are relatively few published studies that recount semantic differential tasks conducted with human participants. Often more emphasis is given, within human trials, to the grouping of similar textures [23], [24]. A process more akin to clustering rather than classification.

III. Method

A. Experimental Setup

A series of artificial textures 3D-printed in ABS plastic were utilised during this experiment. These textures were composed of 1mm cylindrical protrusions ranging in size from $R = 0 - 5\,mm$ in steps of $0.5\,mm$, where R is the radius and distance between each cylindrical pin on the surface. We used a 6-dof robotic arm (ABB, IRB120) to move the neuroTac at a constant velocity (12 mm/s) across the surface of each of the 11 textures for 5000 ms (Fig. 1(a)). This method of interaction was chosen based on neuroscience studies demonstrating the importance of motion in texture recognition [25]. We completed 100 trials per texture to produce 1100 samples from which to train and test our classifiers. For the purpose of training and testing our algorithms, this dataset was split into training and validation sets with ratios of 0.8 and 0.2 respectively. K-fold cross-validation ($k = 10$) was used to further validate our models.

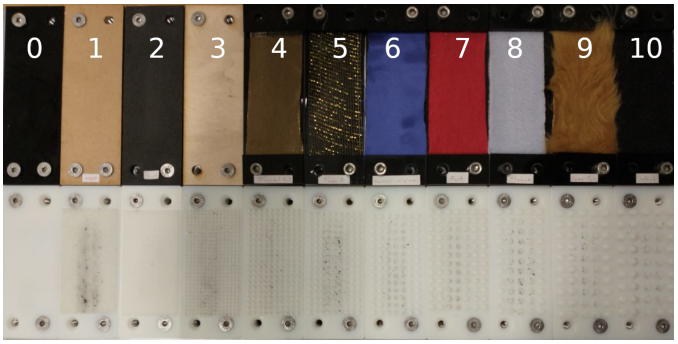

Fig. 2: The top row shows the textures used to create our natural texture dataset. The integer label for each texture is shown, with Table I providing information on the materials used. The bottom row shows our artificial textures, made up of a series of cylindrical pins.

Texture Label	Texture Material
0	Acrylic
1	MDF
2	Foam
3	Plywood
4	Microdot Foil
5	Metallic Mesh
6	Liquid Satin
7	Felt
8	Fleece
9	Fake Fur
10	Wool

TABLE I: Table showing the natural textures trialled within this paper, with related label from dataset.

A dataset was also collected using an assortment of natural textures with the goal of testing any hypothesis derived from the artificial textures, with real-world data. The textures chosen were a subset of the textile and non-textile textures used during initial trials with the neuroTac [5]. Our data collection methodology was kept constant. The number of textures, iterations were also kept constant (10 and 100 respectively) in order to conform with our artificial texture dataset.

B. Temporal Classification

Initial research with the neuroTac utilised a K-nearest neighbours algorithm to classify incoming texture data [5]. During this investigation we further this by testing two additional supervised classification algorithms (Naive Bayes, Multi-layer Perceptron (MLP)).

Original work with the neuroTac looked to investigate different encoding methods for the sensors' spiking output. In this work we utilise the same temporal encoding method to create spike train representations of our input data (Equation 1).

$$Rep(T) = \sum_{n=1}^{N} \sum_{t=T}^{T+\Delta T} t_n^i \tag{1}$$

$Rep(T)$ gives an encoded representation of the incoming spike train, within a moving time window of size ΔT moving in 1 ms increments where t_n^i is a spike time event with index i for pixel n and N is the total number of pixels. This method sums the number of spikes within a time window creating an encoding akin to time-dependent rate coding.

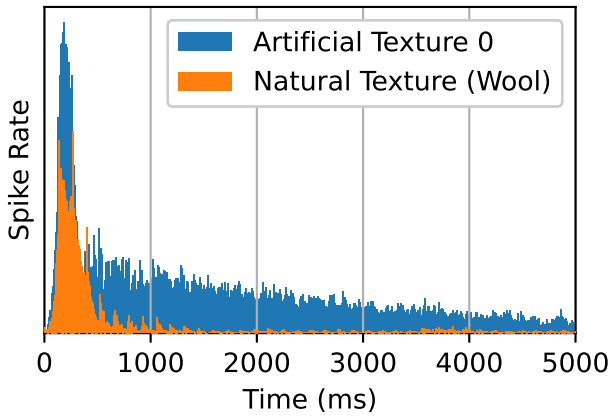

Fig. 3: A comparison of PSTHs from our artificial dataset and natural datasets. As shown in this figure, the artificial textures provided a much higher spike rate than the natural textures. This is consistent across all labels.

We use this time-dependent rate coding to pre-process events before classification which ignores the spatial distribution of events, creating non-overlapping windows of activity for analysis.

The classification of textures with our classical algorithms utilised the firing rate ($Rep(T)$) within these distinct timing windows ($T + \Delta T$). The size of the time window was shown during testing to affect accuracy and was therefore optimised using a Bayesian optimization procedure (Figure 5(a)). The Hyperopt Python module was used for all optimisations within this paper [26].

Figure 3 shows an example histogram of spike intensity over a $5000ms$ data collection sweep ($\Delta T = 10ms$, $n = 100$). A high intensity of spikes can be found within the initial $\approx 500ms$ of the data. This indicates that the initial movement of the sensor encodes more information than the frequent stick-slip events [27] that occur throughout the test. To investigate this further the algorithms were tested with varying sample lengths (t_{in}), as discussed within section IV-A.

C. Spatio-temporal Classification

The data collected by the NeuroTac was analysed in the spatio-temporal domain, via the adaptation and application of the Hierarchy of Event-Based Time-Surfaces (HOTS) pattern recognition architecture, presented within [28].

This method of classification converts event-based data into a subset of fundamental spatial features, occurring around an initial pixel event, in order to form time-surfaces (Figure 4). When any event occurs, a time-surface (square of side length $2rad + 1$, centered on said event) is produced by applying an exponential decay (τ) to recent surrounding events. During training, a set of time-surface prototypes (f) are created. Post

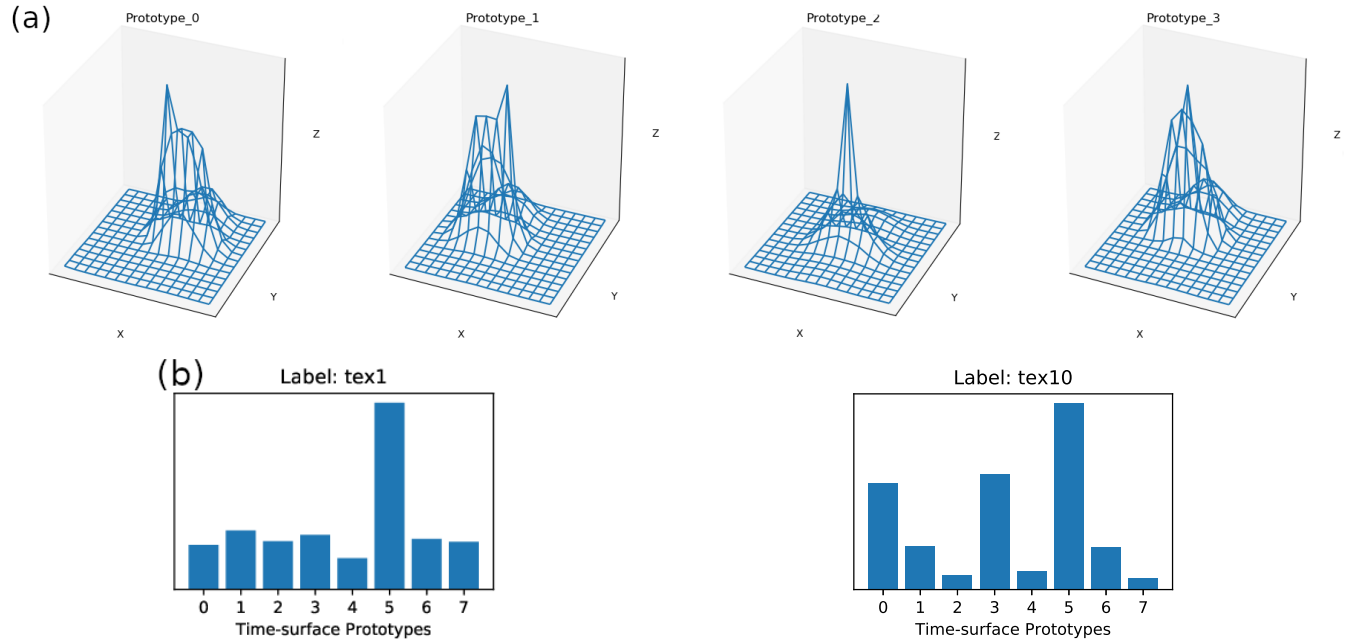

Fig. 4: (a) Example time surfaces formed around a central spiking event. The height of the surface in the z direction indicates the timing of any pixel event in relation to the central spiking event. The initial value of τ was kept constant throughout this experiment at $20us$, with a multiplication factor of $K_\tau = 2$. (b) Histograms showing the differing distributions of fundamental time-surfaces (f) within two natural textures (1 and 10).

training, incoming event streams are converted into a series of surfaces which are in turn compared to the fundamental surface prototypes. The closest matching prototype produces an output event. The density of these fundamental surface outputs within each data label is used to create a histogram of prototype activations. Different textures will thus display signature distributions of time-surface activations (Figure 4 (b)).

HOTS uses a layered structure, similar to conventional multi-layered CNNs, to create the hierarchical model it's named for. The three layered system builds on the initial event data input to describe increasingly complex features. It does so by increasing the size of the time-surfaces both spatially and temporally with each subsequent layer. The following equations describe the network structure:

$$rad_{l+1} = K_{rad} \cdot rad_l \tag{2}$$

$$f_{l+1} = K_f \cdot f_l \tag{3}$$

$$\tau_{l+1} = K_\tau \cdot \tau_l \tag{4}$$

Where K_{rad}, K_f, K_τ are the multiplication factors used to increase the size of the time surface, number of total surface prototypes, and decay constant between layers respectively.

When testing the network, a data point is classified based on the labelled histogram that returns the minimum euclidean distance to the histogram of said data point.

Optimisation of the following parameters was performed on the HOTS architecture. The bounds of the optimisation are described in Table II with the results shown in section IV-B:

Hyperparameter	eps	sam	f_1	rad_1	K_f
Range	1-6	10-22	1-32	1-10	1-3

TABLE II: Hyperparameter ranges for HOTS optimisation. These ranges are the result of initial manual optimisation.

1) eps & sam - For an event to have a time surface built around it, it must first pass through a noise filtering step. An event is filtered out if a neighbouring event fails to occur within radius eps in $\geq sam$ samples.
2) f_1 - The number of fundamental features identified within the first training layer
3) rad_1 - The radius of the time surfaces within the first training layer
4) K_f - Multiplication factor used to increase the number of features identified per layer

For this application we constrained the maximum pixel region for each surface to $rad = 10$ with the aim of creating time surface prototypes that appropriately represent the entire spiking activity around individual taxels.

IV. Results

A. Temporal Classification

The peak accuracies for the temporal classification algorithms can be seen in Table III. These accuracies were derived using the optimisation process described in Fig. 5. A lower relative accuracy for natural textures, when compared

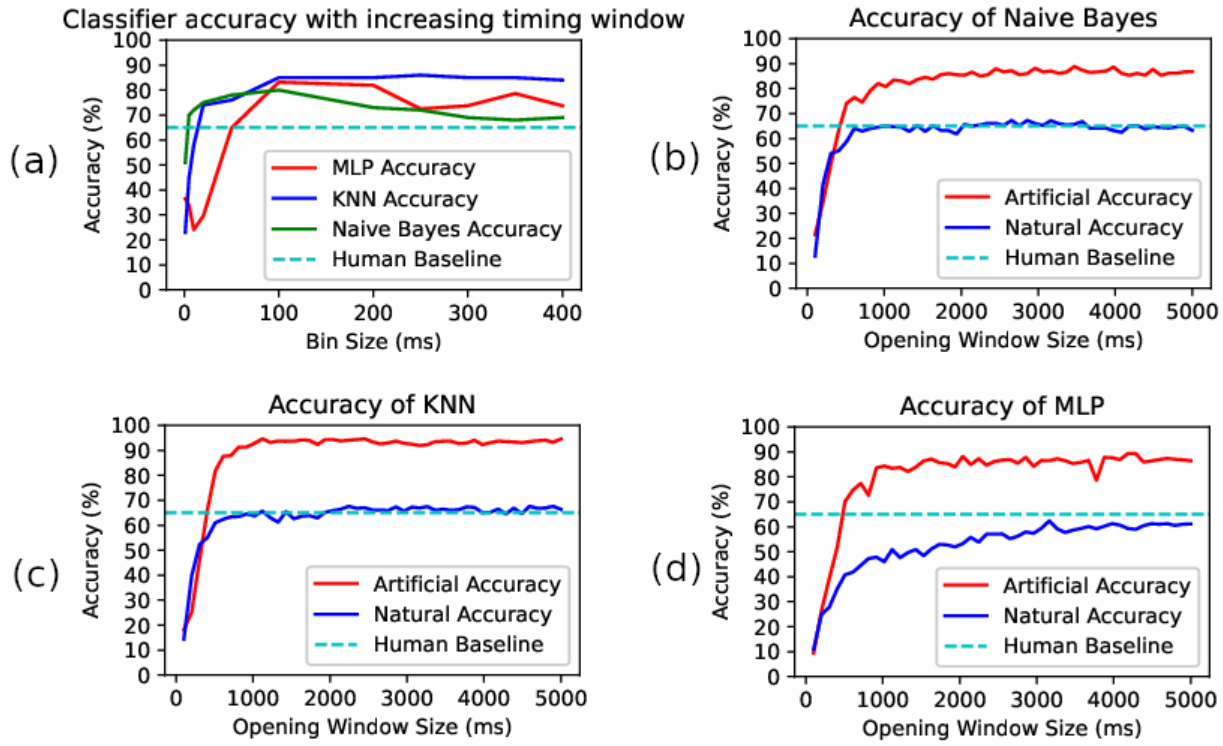

Fig. 5: the optimisation process with the classical machine learning approaches. (a) Relation between the size of the timing window (ΔT) used to calculate spike intensity and texture classification performance for each classical algorithm. (b,c and d) Relation between increasing amount of training data and texture classification performance. Note that a timing window of size $\Delta T = 100ms$ was used to optimise this hyperparameter based on the results of the testing shown in (a)

to the artificial textures, is shown across all classification methods. The uniform nature of the artificial textures generates more regular and repeatable spiking patterns, as evidenced by comparing PSTHs for natural and unnatural textures (Fig. 3). Due to the nature of our spike rate dependant classifiers, this activity hugely contributes towards this discrepancy in accuracy.

A deeper understanding of our classifier results can be derived from the confusion matrices shown in Fig.6. Across classification methods, these matrices report their highest confusion in the middle $(4-6)$ and lower ranges $(0-6)$, for artificial and natural textures respectively.

We postulate that the lower range textures $(0-3)$ of the artificial dataset create distinct taxel oscillations due to friction, reflected in spiking activity. Meanwhile, the large values for R at the higher ranges $(7-10)$ cause taxels to follow repeatable paths across the texture, again leading to easily distinguishable output patterns. It is between these ranges then that the largest confusion is observed, as the spike rates are more similar.

High levels of confusion are seen across methods in the lower range (labels $0-6$) of our natural dataset, as displayed in Fig. 6(b). This confusion is caused by the smoothness of the textures in question. We see largely similar spiking patterns from the sensor, attributed to an observably comparable smoothness, within this range.

To aid in the analysis of our classifiers we devised a time-to-classification metric (t_C). This metric gives an indication of algorithm performance by taking the window of time required for the algorithm to reach an accuracy of within 10% of its peak value. The increase in accuracy of each algorithm over time is shown in Fig.5 with the t_C value presented in Table. III.

Our artificial dataset reports t_C values of between 400 and $700\,ms$. With $\Delta T = 100\,ms$ for these tests, the difference in value between the classifiers can be considered fairly negligible. The natural textures required longer t_C values which is consistent with the decrease in accuracy seen between datasets. Although the Naive Bayes and KNN classifiers reported t_C values similar to those achieved on the artificial dataset, the MLP required $2300\,ms$ of spiking data to confidently classify the textures.

B. Spatio-temporal Classification

Implementation of the HOTS architecture on our artificial dataset resulted in a network capable of classifying neuromorphic texture data with a peak accuracy of 76%. The natural textures produced a lower peak accuracy of 61%, consistent with the drop-off in accuracy seen between datasets using prior methods. The respective confusion matrices are shown in Fig. 6.

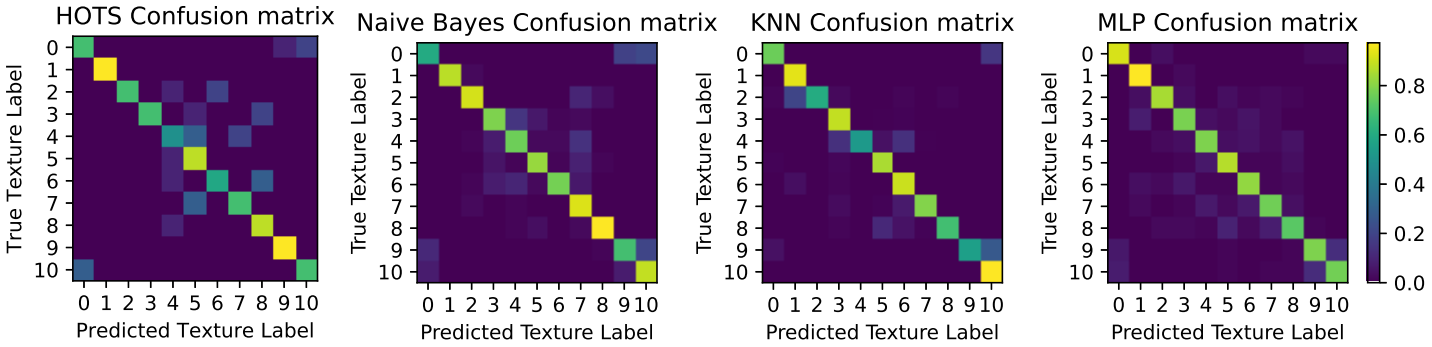

(a) Artificial Textures

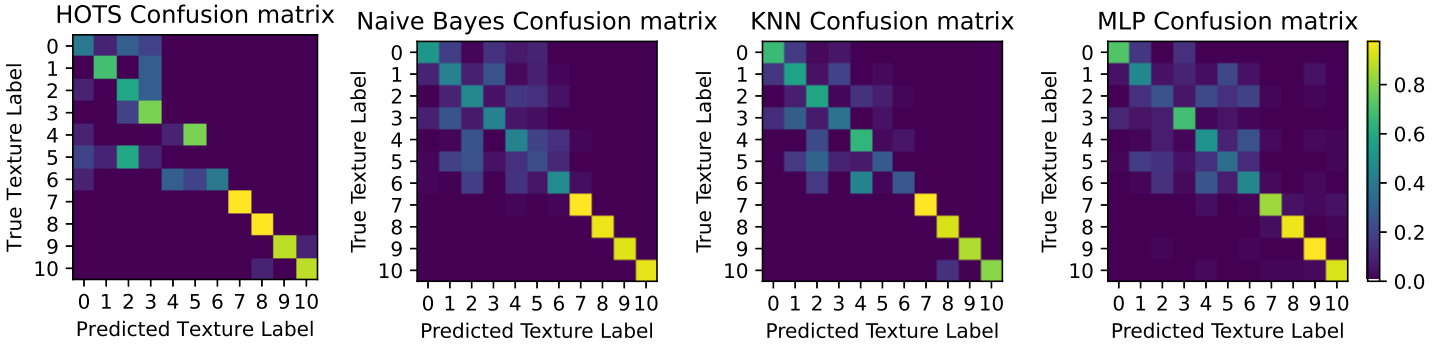

(b) Natural Textures

Fig. 6: Normalised confusion matrices for all texture classification methods trialled within this paper. (a) shows the confusion matrices for the artificial texture dataset, with (b) showing results from the natural dataset.

Dataset	Metric	Algorithm		
		Naive Bayes	KNN	MLP
Artificial	Peak Accuracy (%)	85	91	84
	t_C (ms)	400	500	700
Natural	Peak Accuracy (%)	70.3	68.75	63.8
	t_C (ms)	500	500	2300

TABLE III: Peak accuracies achieved by each supervised algorithm used to classify temporal data

Number of layers	Peak Accuracy (%)	
	Artificial Dataset	Natural Dataset
3	40	50
2	55	53
1	76	61

TABLE IV: Peak accuracy achieved for different number of layers within the HOTS architecture after optimisation.

The peak accuracy of our adapted HOTS architecture was achieved by reducing the number of convolutional layers from the three used within the original publication. Testing with our datasets showed that reducing the number of layers lead to an increase in peak accuracy (Table IV). This was consistent across datasets. This further investigation into network layers was undertaken after initial testing with the three layer system yielded relatively poor results when compared to our temporal domain data ($\leq 50\%$ accuracy). Optimisation processes were run for each differently layered system in order to confirm this trend. A comparatively large increase in accuracy was seen for both the two layer and single training layer systems.

As presented by Lagorce et al. [28] within the original literature, the HOTS architecture identifies more complex features as the number of layers increases. We can assert from our results that during training HOTS is extracting features from our data that, although present, are not intrinsic to specific textures.

V. Discussion and Future Work

The rapid detection of object texture would provide manipulators with a means to autonomously identify objects and avoid noxious surfaces. Implementing these algorithms into active prosthesis would also allow for an improved and more intuitive user experience. For the purpose of this research we used the neuroTac optical tactile sensor to collect a neuromorphic dataset for a set of artificial and natural textures. Our application of supervised machine learning algorithms to this texture data, in the temporal domain, was used to form a baseline from which we could compare a spiking neural network architecture (HOTS), that was able to exploit the spatio-temporal nature of our neuromorphic data.

Texture classification of our datasets in the temporal domain yielded high accuracies (91%), greatly exceeding random chance for this number of textures ($\approx 9.1\%$). This high accu-

racy was maintained across all tested algorithms highlighting the importance of the temporal domain for the classification of these textures. Our findings concur with biological research conducted on Merkel cells and type I Slowly Adapting (SAI) afferents [29], the cells that the tactip head is designed to emulate [30]. The spatio-temporal analysis of our dataset yielded a much lower relative performance (50%) than the temporal domain classification and only increased to a similar performance (76%) when the architecture was stripped back to a single layer. The rapid classification time of $t_C \leq 2300\,ms$ is promising as, with trial lengths of $5000\,ms$, it brings forth the possibility of real-time classification. Future work is planned to investigate online real-time texture classification using SNNs.

The results presented within this paper indicate that simple temporal encoding of spikes from the neuroTac is sufficient to accurately classify textures. The use of our spatio-temporal classifier (HOTS) fails to improve on our temporal classification accuracies. This is true across a dataset of both regular artificial and irregular natural textures. Comparing our results to our psychophysical baseline, we can see that all trialled temporal classification algorithms exceeded our human performance baseline. Despite these high accuracies, higher levels of confusion were observed for smoother textures within our results. Investigations into whether this error can also be seen with human participants are planned as future work in this area. HOTS only began to outperform human participants when stripped back to a single training layer. It must also be noted that HOTS did not exceed our baseline, with any number of layers, when working with natural textures. We speculate that any spatial domain classification may be affected by the morphology of the neuroTac itself, specifically the layout of the taxels within the tip. Although the HOTS architecture did not perform well for this application, further adaptations could lead to its use neuromorphic touch applications such as edge detection or slip.

VI. Conclusions

A series of algorithms have been evaluated for performance in texture discrimination using both temporal and spatio-temporal data from a neuromorphic visuo-tactile sensor. Classifiers utilising the temporal data performed above a human baseline, achieving a peak accuracy of 91%, and were able to rapidly classify both artificial and natural textures ($t_C \leq 2300\,ms$). Our chosen spatio-temporal classifier underperformed when compared to the temporal classifiers ($\leq 76\%$ accuracy). Decomposition of the HOTS spatio-temporal classifier revealed that temporal information encoded in the spike responses to these textures was sufficient for robust classification.

References

[1] T. J. Prescott, M. E. Diamond, and A. M. Wing, "Active touch sensing," 2011.

[2] R. S. Johansson and J. R. Flanagan, "Coding and use of tactile signals from the fingertips in object manipulation tasks," *Nature Reviews Neuroscience*, vol. 10, no. 5, pp. 345–359, 2009.

[3] E. Z. Farsa, A. Ahmadi, M. A. Maleki, M. Gholami, and H. N. Rad, "A low-cost high-speed neuromorphic hardware based on spiking neural network," *IEEE Transactions on Circuits and Systems II: Express Briefs*, vol. 66, no. 9, pp. 1582–1586, 2019.

[4] A. Tavanaei, M. Ghodrati, S. R. Kheradpisheh, T. Masquelier, and A. Maida, "Deep learning in spiking neural networks," *Neural Networks*, vol. 111, pp. 47–63, 2019.

[5] B. Ward-Cherrier, N. Pestell, and N. F. Lepora, "Neurotac: A neuromorphic optical tactile sensor applied to texture recognition," in *2020 IEEE International Conference on Robotics and Automation (ICRA)*. IEEE, 2020, pp. 2654–2660.

[6] K. Ziegler-Graham, E. J. MacKenzie, P. L. Ephraim, T. G. Travison, and R. Brookmeyer, "Estimating the prevalence of limb loss in the united states: 2005 to 2050," *Archives of physical medicine and rehabilitation*, vol. 89, no. 3, pp. 422–429, 2008.

[7] D. De Barrie, R. Margetts, and K. Goher, "Simpa: Soft-grasp infant myoelectric prosthetic arm," *IEEE Robotics and Automation Letters*, vol. 5, no. 2, pp. 699–704, 2020.

[8] G. Tang, A. Shah, and K. P. Michmizos, "Spiking neural network on neuromorphic hardware for energy-efficient unidimensional slam," in *2019 IEEE/RSJ International Conference on Intelligent Robots and Systems (IROS)*. IEEE, 2019, pp. 4176–4181.

[9] M. Davies, "Lessons from loihi: Progress in neuromorphic computing," in *2021 Symposium on VLSI Circuits*. IEEE, 2021, pp. 1–2.

[10] M. M. Iskarous, H. H. Nguyen, L. E. Osborn, J. L. Betthauser, and N. V. Thakor, "Unsupervised learning and adaptive classification of neuromorphic tactile encoding of textures," in *2018 IEEE Biomedical Circuits and Systems Conference (BioCAS)*. IEEE, 2018, pp. 1–4.

[11] A. Song, Y. Han, H. Hu, and J. Li, "A novel texture sensor for fabric texture measurement and classification," *IEEE Transactions on Instrumentation and Measurement*, vol. 63, no. 7, pp. 1739–1747, 2013.

[12] N. Wettels, J. A. Fishel, and G. E. Loeb, *Multimodal tactile sensor*. Springer, 2014, pp. 405–429.

[13] Y. Wu, Y. Liu, Y. Zhou, Q. Man, C. Hu, W. Asghar, F. Li, Z. Yu, J. Shang, G. Liu *et al.*, "A skin-inspired tactile sensor for smart prosthetics," *Science Robotics*, vol. 3, no. 22, 2018.

[14] B. Ward-Cherrier, N. Pestell, L. Cramphorn, B. Winstone, M. E. Giannaccini, J. Rossiter, and N. F. Lepora, "The tactip family: Soft optical tactile sensors with 3d-printed biomimetic morphologies," *Soft robotics*, vol. 5, no. 2, pp. 216–227, 2018.

[15] T. Birkoben, H. Winterfeld, S. Fichtner, A. Petraru, and H. Kohlstedt, "A spiking and adapting tactile sensor for neuromorphic applications," *Scientific Reports*, vol. 10, no. 1, pp. 1–11, 2020.

[16] Z. Yi, Y. Zhang, and J. Peters, "Bioinspired tactile sensor for surface roughness discrimination," *Sensors and Actuators A: Physical*, vol. 255, pp. 46–53, 2017.

[17] A. Drimus, M. Børlum Petersen, and A. Bilberg, "Object texture recognition by dynamic tactile sensing using active exploration," in *2012 IEEE RO-MAN: The 21st IEEE International Symposium on Robot and Human Interactive Communication*, 2012, pp. 277–283.

[18] U. B. Rongala, A. Mazzoni, and C. M. Oddo, "Neuromorphic artificial touch for categorization of naturalistic textures," *IEEE Transactions on Neural Networks and Learning Systems*, vol. 28, no. 4, pp. 819–829, 2017.

[19] M. A. Sivilotti, "Wiring considerations in analog vlsi systems, with application to field-programmable networks," Ph.D. dissertation, California Institute of Technology, 1991.

[20] B. P. Delhaye, E. W. Schluter, and S. J. Bensmaia, "Robo-psychophysics: Extracting behaviorally relevant features from the output of sensors on a prosthetic finger," *IEEE transactions on haptics*, vol. 9, no. 4, pp. 499–507, 2016.

[21] S. Chun, I. Hwang, W. Son, J.-H. Chang, and W. Park, "Recognition, classification, and prediction of the tactile sense," *Nanoscale*, vol. 10, no. 22, pp. 10 545–10 553, 2018.

[22] A. Amini, J. I. Lipton, and D. Rus, "Uncertainty aware texture classification and mapping using soft tactile sensors," in *2020 IEEE/RSJ International Conference on Intelligent Robots and Systems (IROS)*. IEEE, 2020, pp. 4249–4256.

[23] J. A. Fishel and G. E. Loeb, "Bayesian exploration for intelligent identification of textures," *Frontiers in neurorobotics*, vol. 6, p. 4, 2012.

[24] H. Soh, Y. Su, and Y. Demiris, "Online spatio-temporal gaussian process experts with application to tactile classification," in *2012 IEEE/RSJ International Conference on Intelligent Robots and Systems*. IEEE, 2012, pp. 4489–4496.

[25] X. Libouton, O. Barbier, Y. Berger, L. Plaghki, and J.-L. Thonnard, "Tactile roughness discrimination of the finger pad relies primarily on vibration sensitive afferents not necessarily located in the hand," *Behavioural brain research*, vol. 229, no. 1, pp. 273–279, 2012.

[26] J. Bergstra, D. Yamins, and D. Cox, "Making a science of model search: Hyperparameter optimization in hundreds of dimensions for vision architectures," in *International conference on machine learning*. PMLR, 2013, pp. 115–123.

[27] C. Schwarz, "The slip hypothesis: tactile perception and its neuronal bases," *Trends in neurosciences*, vol. 39, no. 7, pp. 449–462, 2016.

[28] X. Lagorce, G. Orchard, F. Galluppi, B. E. Shi, and R. B. Benosman, "Hots: a hierarchy of event-based time-surfaces for pattern recognition," *IEEE transactions on pattern analysis and machine intelligence*, vol. 39, no. 7, pp. 1346–1359, 2016.

[29] S. S. Hsiao, K. O. Johnson, and I. A. Twombly, "Roughness coding in the somatosensory system," *Acta psychologica*, vol. 84, no. 1, pp. 53–67, 1993.

[30] B. Ward-Cherrier, N. Pestell, L. Cramphorn, B. Winstone, M. E. Giannaccini, J. Rossiter, and N. F. Lepora, "The tactip family: Soft optical tactile sensors with 3d-printed biomimetic morphologies," *Soft robotics*, vol. 5, no. 2, pp. 216–227, 2018.